A mechanism that produces a dichotomy in melt pond coverage in sea ice floes

Predrag Popović[1] and Dorian S. Abbot[1]

[1]Department of Geophysical sciences, University of Chicago, Hinds Geophysical Sciences, 5734 S. Ellis Ave., Chicago, IL 60637

Correspondence to: Predrag Popović (ppopovic@uchicago.edu)

Abstract. Late in the melt season, sea ice floes in the Arctic have been observed to exhibit a large range in melt pond coverage, from heavily ponded to almost pond free. Some of these observations are consistent with a bimodal distribution in pond coverage with few intermediately ponded ice floes. We present a model for the evolution of melt ponds on sea ice floes in which conservation of hydrostatic balance in response to melt creates an unstable fixed point in pond coverage: if the initial pond coverage is below a threshold value the floe becomes unponded, and if it is above the threshold the floe becomes heavily ponded. Whether the fixed point is physically realistic depends on the differential melting rates of different points on the ice: ice at the perimeter of ponds needs to melt sufficiently slower than bare ice on average. Interestingly, this shows that the melting behavior of the narrow boundary between bare ice and melt ponds can govern the melt pond evolution of the entire ice floe. Since melt pond coverage is one of the key parameters controlling the albedo of sea ice, understanding the mechanisms that control the distribution of pond coverage will help us improve large-scale model parameterizations and sea ice forecasts in a warming climate.

1 Introduction

Over the past forty years, Arctic summer sea ice extent has reduced by 50 percent, making it one of the most sensitive indicators of man-made climate change (Serreze and Stroeve, 2015; Stroeve et. al., 2007; Perovich and Richter-Menge, 2009). This rapid decrease was at least partially due to the ice-albedo feedback (Zhang et. al., 2008; Screen and Simmonds, 2010; Perovich et. al., 2007). Moreover, if the ice-albedo feedback is strong enough it could lead to instabilities and abrupt changes in ice coverage in the future (North, 1984; Holland et. al., 2006; Eisenman and Wettlaufer, 2008; Abbot et al., 2011). The albedo of ice is strongly affected by the presence of melt ponds on its surface (Eicken et. al., 2004; Perovich and Polashenski, 2012; Yackel et. al., 2000). Therefore, understanding the evolution of melt ponds is essential for understanding the ice albedo feedback, and consequently, the evolution of Arctic sea ice cover in a warming world.

Another important effect of melt ponds is their impact on ocean biology underneath sea ice. Melt ponds transmit up to an order of magnitude more sunlight than bare ice (Frey et. al., 2011; Perovich, 1996). In a warming world, melt pond fractional coverage is expected to increase (Holland et. al.,

2012; Landy et. al. 2015) leading to an increase in light intensity under the ice cover (Nicolaus et. al. 2012). This should cause a large increase in primary production beneath the ice, and hence,

30 accelerate the entire Arctic ecosystem. Already, phytoplankton blooms of unprecedented proportions have been observed under Arctic sea ice (Arrigo et. al. 2012).

Accurate melt pond parameterizations must be incorporated into Global Climate Models (GCMs) to improve their sea ice forecasts and ecosystem impacts (Flocco et. al. 2010; Holland et. al. 2012; Pedersen et. al. 2009). The main difficulties with understanding the pond evolution are that it is

35 nonlinear and that it is the result of a variety of different physical processes operating on a range of length and time scales. Typically, the evolution of pond coverage on first year ice proceeds in a fairly consistent manner (Polashenski et. al. 2012; Perovich et. al. 2003; Landy et. al. 2014; Fetterer et. al. 1998; Webster et. al. 2015). First the ponds grow quickly while the ice is impermeable. Next they drain quickly and pond coverage shrinks as the ice transitions from impermeable to permeable.

40 Then the ponds grow slowly while the ice is permeable and pond water remains at sea level. Finally, the ponds either refreeze or the floe breaks up.

In this paper we will explore the possibility that pond evolution on a particular floe can deviate from the above pattern. Specifically, we will be concerned with the evolution of the ice floes while the ice is permeable. During the SHEBA mission of 1998, it was observed that first year ice can come

45 in two flavors: one where it becomes heavily ponded and another where it becomes almost unponded (Perovich et. al. 2002). Figure 1 shows an example of this behavior in two photographs that were both taken on June 15th 1998 relatively close to each other. One shows heavily ponded ice while the other only slightly ponded ice. We should note that despite this qualitative evidence, the dichotomy in pond coverage has not been confirmed by extensive observations. An alternative possibility is

50 that the pond coverage distribution is unimodal with a long tail towards low pond fractions, which we will consider later in this paper. Nevertheless, Perovich et. al. (2002) suggested that there is a mechanism driving the ice into one of these two states. The nature of this mechanism, as well as its role in the total albedo of the ice pack have not been explained.

The purpose of this paper is to present a minimal conceptual model that is capable of producing

55 a pond coverage dichotomy. By considering different ways to melt permeable floating ice, we show that pond coverage can either increase or decrease with time depending on the initial pond coverage. We also show that this threshold behavior depends on the details of interaction between ice and pond water, meaning that further observations and modeling are required to establish its physical relevance. Even if the conditions for the dichotomy are not met and ponds always grow, our model

60 can still produce a large range of pond fractions because the timescale of the governing equation can span a large range of values. If observations show that our bimodal model is correct, it will allow us to identify the roles played by different energy fluxes and the interaction between ice and pond water in creating the dichotomy in melt pond coverage. This will, in turn, help us predict which state of pondedness will become preferred under a global warming scenario.

65   This paper is organized in the following way. In section 2 we provide a physical explanation of a mechanism that gives rise to a dichotomy in sea ice pondedness. In section 3 we use this understanding to build a single-column model for the evolution of pond coverage, we analyze it using some realistic parameters, and then we generalize it to a 2D surface. In section 4 we discuss the physical processes that could enable the conditions under which the bimodal mechanism is operable. In sec-

70 tion 5 we discuss additional problems the model might face and suggest other possible explanations for the observations. Finally in section 6 we summarize our results.

2   How differential melt rates can produce a melt pond coverage dichotomy

We first consider the following thought experiment to show that some points on the surface of floating ice can move upwards as the ice is melting. Imagine a uniform slab of completely permeable ice floating in water and melting only by absorption of sunlight from above. Suppose that most of the

75 ice is melting at some rate, but there is a particular place on the ice surface that reflects all incident sunlight, and does not melt at all. The ice will thin everywhere except at this special place, where the thickness will remain unchanged. Since the ice is permeable, all the melt water will be removed to the ocean, and to compensate for the loss of mass above sea level the slab has to float upwards.

80 This moves the special region that is not melting to a higher elevation than it started at (Fig. 2a).

    If the situation were the same in every respect except the melt were occurring below sea level, loss of mass below sea level would be followed by sinking of the ice, and all the points on the ice surface would move downwards at the same rate. The non-melting region would be no different, and would move downwards as well (Fig. 2b). This shows that melting above and below sea level

85 have different effects on the motion of points on the ice surface. If the ice is melting both above and below sea level, the non-melting region could in principle move either upwards or downwards, and the condition that it remains at its starting location is:

$$\frac{dm_{\mathrm{aboveSL}}}{dm_{\mathrm{belowSL}}} = \frac{\rho_{\mathrm{w}} - \rho_{\mathrm{i}}}{\rho_{\mathrm{i}}} \,, \tag{1}$$

where ρ_{w} and ρ_{i} are the densities of water and ice respectively, and $dm_{\mathrm{above/belowSL}}$ stands for mass

90 removed above or below sea level. We will call motion that is the result of losing mass above or below sea level the "rigid body" movement, since it represents the motion of the floe as a whole (Fig. 3a). An ice floe is naturally not a rigid body, but up to its flexural wavelength we can approximate it as such. Even though in this paper we assume the entire floe moves as a rigid body, distant regions of the floe could in fact be unrelated.

95   Next we consider the case where a small low-albedo surface patch is surrounded by perfectly reflective ice. In this case, the amount of mass removed above sea level would be insignificant compared to the total mass of the floe, and its rigid body response would be negligible. Nevertheless, the special region would move downwards at a constant rate (Fig. 3b, Fig. 2c). We will call this type of motion "local", since, unlike the rigid body movement, it depends on local characteristics

100   of a particular point (region). Unlike rigid body displacement, local displacement can only point
downwards for the points on the surface of the ice.

When different regions of ice melt at different rates, the total vertical motion of a point on the
ice surface is a combination of local motion due to melting of the ice at that point, and rigid body
motion due to melting of the surrounding ice. Depending on how quickly the ice melts locally and
105   how much melt is occurring above and below sea level, a point on the ice surface may either move
downwards or upwards. We know, however, that during the melt season the ice is thinning, which
means that, overall, the freeboard (average height of the ice surface above sea level) is sinking. This
means that on average, points on the ice surface need to be moving downwards. However, some
points could be moving upwards if they melt slower than average.

110   If the ice is permeable, the surface of all melt ponds must be at sea level. Therefore, the only
way for the ponds to grow is if the points on ice near the pond perimeter, which are slightly above
sea level, move downwards to below sea level. Likewise, the ponds can only shrink if points on the
perimeter move upwards to above sea level. Above we explained how it is possible for points to
move upwards if (1) they melt slowly enough compared to the rest of the points on the ice surface
115   above sea level and (2) if melting above sea level is strong enough compared to melting below sea
level.

The first condition requires that the points on the pond perimeter melt slower than the rest of the
points on the ice surface above sea level. This means that they must be special in some way. In
fact, they are unique for at least two reasons: (1) they are all near sea level and (2) they are located
120   at the ice-water interface. This special nature potentially provides them with unique topographical,
thermal, and optical properties, which can influence their rate of melt. For now, we will simply note
that the melt rate at these points depends on detailed physics and could, on average, be either larger or
smaller than the melt rate of the surrounding ice. In section 4 we discuss some possible mechanisms
that could produce a decrease in the rate of melt for the points on the pond edge. For now we will
125   proceed assuming that it is possible for these points to melt slowly enough to allow them to move
upwards.

The second condition requires that melting above sea level is strong enough compared to melting
below sea level. Since ponds are at sea level, melting ice beneath the ponds removes mass below sea
level inducing a downward motion of the floe that tends to grow the ponds. Melting bare ice, on the
130   other hand, induces an upward motion of the floe, shrinking the ponds. This leads to a competition
of two opposing effects: melting bare ice increases the bare ice fraction at the expense of melt ponds,
while melting ponded ice grows the ponds at the expense of bare ice. The larger the pond fraction is,
the larger their tendency to grow will be and the smaller their tendency to shrink will be. Therefore,
there could be a particular value of pond fraction where melting above sea level is just strong enough
135   to compensate for melting below sea level and melting locally at the pond perimeter so that ponds
neither grow nor shrink. If pond coverage is higher than this value, melting below sea level will

be strong enough to make the ponds grow. If the pond coverage is lower than this value, melting above sea level will win, and the ponds will shrink. In this way a dichotomy in pond coverage can be produced.

3 A single-column model for the evolution of pond coverage can produce a pond coverage dichotomy using realistic parameters

In the previous section we saw that depending on the magnitudes of total melting above and below sea level, and local melting at the pond perimeter, ponds can either shrink or grow. We will now quantify these contributions and construct a single-column model to describe the evolution of melt pond fraction. The single-column model will be represented by a nondimensionalized equation in which the rate of change of pond fraction is a function of pond fraction.

Following the ideas from the previous section, we divide the total rate of change of vertical position of the point r on the surface of the ice, $\frac{ds_\text{tot}}{dt}(r)$, into a contribution from the rigid body motion, $\frac{ds_\text{rigid body}}{dt}$, and a contribution from the local melting, $\frac{ds_\text{loc}}{dt}(r)$

$$\frac{ds_\text{tot}}{dt}(r) = \frac{ds_\text{rigid body}}{dt} + \frac{ds_\text{loc}}{dt}(r).$$ (2)

Rigid body displacement is determined by the total energy used for melting the ice above or below sea level. It can be split into three contributions: melting bare ice from above ($\frac{ds_\text{bi}}{dt}$), melting ponded ice from above ($\frac{ds_\text{mp}}{dt}$), and melting the ice bottom by the deep ocean heat flux or energy deposited in the ocean by transmitting sunlight through leads and ice ($\frac{ds_\text{bot}}{dt}$). Melting bare ice corresponds to melting above sea level, while melting ice under melt ponds and melting the ice bottom correspond to melting below sea level. The total rigid body displacement is the sum of these three contributions, as follows

$$\frac{ds_\text{rigid body}}{dt} = \frac{ds_\text{bi}}{dt} + \frac{ds_\text{mp}}{dt} + \frac{ds_\text{bot}}{dt}.$$ (3)

If we remove a layer of ice of volume dV below sea level, then hydrostatic adjustment reduces the volume of ice above sea level by $dV' = \frac{\rho_\text{w}-\rho_\text{i}}{\rho_\text{w}}dV$. Conversely, if we remove a layer of ice of volume dV above sea level, then the volume of ice below sea level has to reduce by $dV' = \frac{\rho_\text{i}}{\rho_\text{w}}dV$. If the melted layer has a surface area of A_0, then we can express the volume of the melted region via the flux of energy, F, used for melting the layer, $dV = \frac{FA_0 dt}{L}$, where L is the latent heat of melt in units of energy per volume. When ice floats up or down by $ds_\text{rigid body}$ due to hydrostatic adjustment, the change in volume above or below sea level will be proportional to the area of bare ice (A_bi), and not to the total area of the floe (A). This is because bare ice is above sea level meaning that ice can only cross sea level in these regions, given that the vertical displacement is small enough (Fig. 4).

Therefore, we have $dV' = A_{\text{bi}} ds_{\text{rigid body}}$. Using the relation between dV and dV', we can infer that

$$
\frac{ds_{\text{bi}}}{dt} = \frac{\rho_i}{\rho_w} \frac{\overline{F}_{\text{bi}}}{L} ,
$$
$$
\frac{ds_{\text{mp}}}{dt} = -\frac{\rho_w - \rho_i}{\rho_w} \frac{A_{\text{mp}}}{A_{bi}} \frac{\overline{F}_{\text{mp}}}{L} ,
$$
$$
\frac{ds_{\text{bot}}}{dt} = -\frac{\rho_w - \rho_i}{\rho_w} \frac{A}{A_{\text{bi}}} \frac{\overline{F}_{\text{bot}}}{L} , \tag{4}
$$

170   where the positive direction is upwards, $\overline{F}_{\text{bi}}$ is the energy flux used for melting bare ice averaged over all the regions of bare ice, $\overline{F}_{\text{mp}}$ is the energy flux used for melting ponded ice averaged over all the regions of ponded ice, and $\overline{F}_{\text{bot}}$ is the energy flux used for melting the ice bottom averaged over the ice bottom. Averaged fluxes depend on parameters such as the average insolation on the floe, average albedo, average longwave, sensible, latent and bottom heat fluxes. Note that melting

175   above sea level produces a larger change in the rigid body displacement than melting below sea level because of the effects of buoyancy ($\frac{\rho_i}{\rho_w} \approx 0.9$, as opposed to $\frac{\rho_w - \rho_i}{\rho_w} \approx 0.1$).

We can determine the local melt rate from the flux of energy, $F(\boldsymbol{r})$, used for melting the ice at a point $\boldsymbol{r}$ on the surface

$$
\frac{ds_{\text{loc}}}{dt} = -\frac{F(\boldsymbol{r})}{L} \tag{5}
$$

180   The positive direction is again defined as upwards. The local flux depends on parameters such as local albedo, local insolation, longwave, sensible and latent heat fluxes, and the slope of the ice at that point. The flux $F(\boldsymbol{r})$ averaged over all the points on the surface of the ice above sea level has to equal $\overline{F}_{\text{bi}}$, since this is the average flux above sea level. This means that the displacement due to local melting and the rigid body displacement due to melting bare ice are related by

185   $$
\frac{ds_{\text{bi}}}{dt} = -\frac{\rho_i}{\rho_w} < \frac{ds_{\text{loc}}}{dt}(\boldsymbol{r}) > , \tag{6}
$$

where $< ... >$ stands for averaging over all the points on the ice surface above sea level. Since ponds can only shrink or grow through the motion of points on their perimeter, instead of assessing $\frac{ds_{\text{loc}}}{dt}(\boldsymbol{r})$ for a general point, we will consider the average rate of motion due to local melting averaged over all the points on the perimeter of the ponds, $< \frac{ds_{\text{loc}}}{dt}(\boldsymbol{r}) >_{\text{perim}}$, effectively reducing our model to a

190   "single column." Because of the relation between melting bare ice and local melting (Eq. (6)), we will represent local melting at the pond perimeter with the term

$$
< \frac{ds_{\text{loc}}}{dt} >_{\text{perim}} = -k \frac{\overline{F}_{\text{bi}}}{L} , \tag{7}
$$

where k is a nondimensional number that summarizes all of the detailed physics of the pond boundary layer that we are not taking into account. Depending on specific physical conditions, k could be

195   either greater than or less than one. Here we will take k to be constant, but in reality it could be a function of any of the parameters involved, as well as a function of time.

Lastly, we need to relate the displacements to the change in area of the melt ponds (Fig. 5). In reality this would depend on the rates of melt and the slope between ice and pond water at every point along the boundary, and it would change with time. Here we will assume there is some average slope of ice at the pond edge, α, and that it is representative of every point along the edge at all times. This is clearly a very restrictive approximation but ultimately does not strongly affect our results. We can then relate the total displacement of the perimeter points to the change in area of the melt ponds by

$$dA_{\mathrm{mp}} = -ds_{\mathrm{tot}} \cot(\alpha) P \,, \tag{8}$$

where P is the total perimeter of the ponds. Here we are neglecting the change in pond coverage as a result of new ponds forming. If we imagine an ice floe of area A covered with ponds of typical linear size l_0 (small ponds which might or might not be interconnected), such that pond boundaries define a curve similar to a fractal with the fractal dimension 2 (Hohenegger et. al., 2012), then the perimeter P has to scale as $P = \frac{A}{l_0} p_0(A_{\mathrm{mp}})$. The function $p_0(A_{\mathrm{mp}})$ is dimensionless, positive, of the order one, and goes to zero as area of melt ponds, A_{mp}, approaches 0 or A (the perimeter of the ponds vanishes if there are no ponds, or if the whole floe is a single pond). We estimate this function in appendix A. The reciprocal of the constant l_0, $\frac{1}{l_0}$, represents the total length of the perimeter of the ponds per unit area of the ice at the value of pond coverage for which $p_0(A_{\mathrm{mp}}) = 1$ (in our case this is also the maximum for the function $p_0(A_{\mathrm{mp}})$). We can now convert the equation for the displacement into an equation for the pond fraction, thus completing our single-column model. For mathematical convenience, we will use the bare ice fraction, which is defined as one minus the pond fraction. The nondimensionalized equation obtained by combining equations 2, 3, 4, 7, and 8 reads

$$\frac{dx}{d\tau} = \frac{p_0(x)}{x} \left(x - x_0 \right) \,, \tag{9}$$

where x is the bare ice fraction, and $\tau = \frac{t}{T}$ is the nondimensional time. The timescale T and the parameter x_0 are defined as follows:

$$T = \frac{l_0 L \rho_{\mathrm{w}} \tan(\alpha)}{(\rho_{\mathrm{i}} - k\rho_{\mathrm{w}})\overline{F}_{\mathrm{bi}} + (\rho_{\mathrm{w}} - \rho_{\mathrm{i}})\overline{F}_{\mathrm{mp}}} \,,$$
$$x_0 = \frac{(\rho_{\mathrm{w}} - \rho_{\mathrm{i}})(\overline{F}_{\mathrm{mp}} + \overline{F}_{\mathrm{bot}})}{(\rho_{\mathrm{i}} - k\rho_{\mathrm{w}})\overline{F}_{\mathrm{bi}} + (\rho_{\mathrm{w}} - \rho_{\mathrm{i}})\overline{F}_{\mathrm{mp}}} \,, \tag{10}$$

Equation (9) has a fixed point at $x = x_0$. Since $p_0(x) > 0$, the fixed point is unstable (Strogatz, 2000). This means that for $x < x_0$, the floe gets more and more ponded, while for $x > x_0$ the pond coverage shrinks. A phase portrait for bare ice fraction is shown in figure 6.

The main issue with Eq. (9) is that x_0 is by no means constrained to be greater than zero or less than one, a condition necessary for it to be physically meaningful. This requires

$$0 < x_0 < 1 \iff \frac{k\overline{F}_{\mathrm{bi}} + \frac{\rho_{\mathrm{w}} - \rho_{\mathrm{i}}}{\rho_{\mathrm{w}}}\overline{F}_{\mathrm{bot}}}{\frac{\rho_{\mathrm{i}}}{\rho_{\mathrm{w}}}\overline{F}_{\mathrm{bi}}} < 1 \,. \tag{11}$$

If x_0 is greater than one, there is no fixed point and bare ice fraction always decreases. Guided by analogy, one might assume that negative x_0 means that bare ice fraction will always increase. This is, however, not the case. During the melt season ($\overline{F}_{\mathrm{mp}} > 0$ and $\overline{F}_{\mathrm{bi}} > 0$), the only way for $x_0 < 0$ is for the denominator in Eq. (10) to be negative. This is the case if k is large enough. However, since both x_0 and T share the same denominator, negative x_0 would necessarily imply a negative timescale T. Even though in this case the right hand side of Eq. (9) would be positive for all possible values of x, since the timescale is negative, the parameters x_0 and T would have to be redefined with an additional minus sign, making the rate of change of bare ice fraction negative for all values of x. This means that bare ice fraction would in fact always decrease. There is a discontinuity at $x_0 = 0$, since in the case $x_0 \to 0^+$ bare ice fraction always increases, and $x_0 \to 0^-$ bare ice fraction always decreases.

The numerator in Eq. (11) represents the sum of the local and bottom melting terms, while the denominator is the bare ice melting term. In order for the fixed point to be physical, upward motion due to melting bare ice from above needs to be greater than combined downward motion induced by local melting at the perimeter and melting from the bottom. The bottom energy flux is roughly of the same order of magnitude as the surface energy flux (Perovich et. al., 2003, 2011). However, because it is weighted by $\frac{\rho_{\mathrm{w}} - \rho_{\mathrm{i}}}{\rho_{\mathrm{w}}}$, it is roughly 9 times less effective in moving the points on the ice surface than surface melting is, so that in some cases we might consider it small. If the contribution from bottom melting is negligible, then the condition 11 reduces to

$$0 < x_0 < 1 \Longleftrightarrow k\frac{\rho_{\mathrm{w}}}{\rho_{\mathrm{i}}} < 1 \tag{12}$$

In this case, for the fixed point to be between 0 and 1, k needs to be less than 0.9, meaning that the perimeter needs to melt 10% slower than bare ice on average. If we include bottom melting, and assume it is of the same magnitude as surface melting, points at the perimeter would have to melt roughly 20% slower than bare ice (k less than 0.8).

The timescale of Eq. (9), T, is unconstrained since it depends on the slope of the ice-water interface, $T \propto \tan(\alpha)$. This is because if the ice-water interface slope is small, any small perturbation of the freeboard height will lead to large changes in pond area, while if the interface is steep, motions of the points near the perimeter would produce little change in area. The timescale also depends on the constant l_0, which we cannot constrain well at this point, but since pond patterns are variable at length scales of meters, we will assume here that $l_0 \approx 1\mathrm{m}$. The flux of energy used for melting bare ice in mid-summer is of the order of $50\mathrm{Wm}^{-2}$, the flux used for melting ponded ice is of the order of $70\mathrm{Wm}^{-2}$, and ocean flux is roughly $30\mathrm{Wm}^{-2}$ (Perovich et. al., 2003, Maykut and Mcphee, 1995). Using these values, we get the timescale as,

$$T \approx \left(0.8 \text{ years }\right)\tan(\alpha) \tag{13}$$

We see that for the timescale to be of the correct order of magnitude, namely 30 to 90 days, the slope of the ice at the pond perimeter needs to be roughly $5^o - 15^o$, which we believe is reasonable.

However, there exist significant uncertainties in calculating the timescale (e.g. in estimating l_0), and
after careful examination of the parameters, the timescale we found in Eq. (13) could prove to be
appreciably off. Nevertheless, we do not believe that this is particularly damaging to the theory
presented here. In the case of $k = 1$ points on the pond perimeter melt at the same rate as points on
bare ice, and our model should reasonably describe pond growth by freeboard sinking. Since it has
been confirmed that ponds can grow significantly by sinking of the freeboard in a matter of days
(Landy et. al., 2014; Polashenski et. al., 2012), a potential discrepancy between the model timescale
and the length of the melt season would be purely due to the crudeness of the model, and not due to
insignificance of the presented mechanisms.

We plot numerical solutions to Eq. (9) in figure 7. If k is small enough, after a period of about 30
days floes that started off with similar bare ice fractions end up being quite different. Since the initial
pond coverage depends on premelt snow and ice topographies, and can vary greatly (Eicken et. al.,
2004; Scott and Feltham, 2010), we explore how a full distribution of initial pond coverage changes
through time in Figure 8. We start with an ensemble of floes each having a bare ice fraction drawn
from some initial distribution, and then evolve it according to Eq. (9). If the ponds grow simply by
sinking of the freeboard ($k = 1$, panel a), after some time, the floe distribution becomes very narrow
with a short tail, and a well-defined pond fraction. This is contrary to the observation that there is
a considerable number of floes with low pond coverage. On the other hand, a bimodal distribution
is easily produced if a fixed point splits the initial distribution into two parts (panel b). Even if the
initial distribution is bimodal, it can be difficult to produce a clear bimodal evolved distribution
when the ponds grow simply by freeboard sinking (panel c). Melt pond coverage might also be
unimodally distributed with a long tail. Within our framework, long tailed unimodal distributions
can be produced if the initial distribution is close to a fixed point (panels d to f). Near a fixed point,
dynamics slow down, so that floes that start with pond coverage close to a fixed point will take a
much longer time to experience a change in pond coverage than those that start farther away. Panel
d) shows how a long tailed distribution is created when the initial distribution is close to a fixed point,
but is not split by it. Besides the fixed point at $x = x_0$, there also exists a trivial fixed point at $x = 1$
(Fig. 6). This means that even if $x_0 > 1$, a long tailed distribution can be produced if a significant
number of the floes start off nearly pond free (panel e). If the initial distribution is bimodal, and one
of the modes is close to $x = 1$, the end distribution will be bimodal (panel f), but the structure of this
distribution will be quite different to that shown in panel b. These results could provide a basis for
observational tests of the model: by observing the change in pond coverage distribution over time,
one could surmise whether there exists a nontrivial fixed point. However, the results shown here
should not be overinterpreted given that we have neglected the details of many processes, such as
formation of new ponds, spatial and temporal variations in α and k, estimation of the function $p_0(x)$,
etc., that could have important effects on the detailed evolution of pond coverage.

We can easily generalize our single-column model to two dimensions by writing the equation for ds_{tot} for each point on a 2D grid. We did this by specifying the local melting rate for each point: $ds_{\mathrm{tot}}(\boldsymbol{r}, A_{\mathrm{mp}}) = ds_{\mathrm{bot}}(A_{\mathrm{mp}}) + ds_{\mathrm{mp}}(A_{\mathrm{mp}}) + ds_{\mathrm{bi}} + ds_{\mathrm{loc}}(\boldsymbol{r})$, where $\boldsymbol{r}$ and A_{mp} stand for the position vector and the area of melt ponds respectively. We generated a 2D surface as described in appendix A. We set sea level to $z = 0$, and defined ponds as the regions of the surface with elevation below zero. We prescribed energy fluxes globally, but prescribed albedo individually at each point. The albedo of melt ponds was a function of pond depth, while the albedo of ice was constant. A narrow lip around the pond edge had a slightly higher albedo than bare ice. Knowing the fluxes and the albedo allowed us to calculate the displacements and evolve the system in time. Figure 9 shows two points in time for two surfaces identical in every respect apart from the upper one being initially slightly more ponded than the lower one.

We see that the floes evolve just as we would expect. Starting with pond coverage larger than some threshold value, a floe would get heavily ponded, while a floe starting below this threshold will remain at low pond coverage. A noticeable difference between this and the single-column model is that in the 2D case, the ponds cannot disappear. They shrink a little, and then they get deeper and deeper without shrinking or growing. This is because only the points near the pond perimeter melt slower than bare ice. The points on the bottom of deep ponds melt faster than bare ice, and therefore, cannot move upwards.

4 Physical mechanisms that could lead to a decreased melt rate at the pond boundary

We saw that in order for the mechanism described in this paper to be realistic, the points near the pond edge need to melt slower than bare ice far away from the ponds. Let us now consider some plausible physical processes which might give these points such a property. This is by no means an exhaustive list, and each of these mechanisms can only be operational under certain conditions. Furthermore, there could be mechanisms forcing the pond edge points to melt faster than points on bare ice. Nevertheless, it is encouraging that there are straightforward mechanisms that could cause a slower melt rate at the pond edge. Since detailed physics, possibly operating on microscopic scales, determines the difference in melting rates, more experiments, observations, and detailed theories are needed to determine whether this is the mechanism responsible for the pond coverage dichotomy in Arctic sea ice suggested by observtions.

a) The diurnal cycle could be such that the ice melts during some part of the day and freezes during another, with net melting occurring on average. Then, since ice is permeable, meltwater created during the melting part of the day above bare ice could seep through the ice. During the freezing part of the day, there would be no water to freeze on bare ice, but there would be an abundance of water at the pond edge which could freeze, thus making the net melting rate at the pond boundary lower than average net melting rate on bare ice (Fig. 10a).

b) Arctic sea ice is often loaded with dark impurities, such as dust, black carbon or sediments (Nürnberg et. al., 1994; Pfirman et. al., 1990; Perovich et. al., 1998; Light et. al., 1998; Tucker et. al., 1999). Dark particulates can significantly lower the abedo of the ice. Even if the ice appears clean, it can have trace amounts of dark particulates that can lower the albedo by $5 - 10\%$ in the visible spectrum. In some regions of the Arctic, up to 50% of sea ice can be significantly loaded with dark particulates. If the ice has a significant amount of impurities, bare ice could stay covered in dirt, whereas water could wash away the dust on the edge of the ponds, exposing the more reflective white ice. In this way, the pond edge could have a significantly lower melt rate than the rest of the ice (Fig. 10 b).

c) Points at the pond edge are necessarily at a lower elevation than any of the points on bare ice. This would mean that the pond edge always gets less sunlight compared to bare ice, since it is partially shaded by it. This effect is strongest if the ice is rough, the slope is steep, and the Sun is low (Fig. 10 c). For ice slopes at the perimeter of around 30° and perfectly level bare ice, throughout most of the Arctic, for most of the time, the perimeter points would experience at least some shadowing. The effect would be lessened if the conditions are cloudy. If the ice is rough, features such as ridge sails could provide effective shading, and this effect could be especially prominent. However, we saw that for changes in pond area to occur on relevant timescales, the slope of the ice at the pond edge has to be small (of the order of $5^o - 15^o$). This could mean that for most cases of interest, the shadowing effect is quite small.

5 Discussion

Our single-column model assumed the slope of the ice at the ice-water interface is constant in both space and time, and does not vary with pond depth. This clearly unrealistic assumption led to the possibility of ponds disappearing. We believe it is unlikely that this occurs in nature. As exemplified by the 2D generalization of the single-column model, our mechanism was able to make the ponds shrink a little, but could not make them disappear. For the ponds to disappear, points on the pond bottom have to move upwards, that is, they have to melt slower than points on bare ice. This might be true for points near the pond edge where the water is shallow, and the effect of increased sunlight absorption by water is minimal (although even a very shallow layer of water can decrease the albedo (Makshtas and Podgorny, 1996)). Albedo generally decreases with depth exponentially up to some critical depth (Morassutti and Ledrew, 1996), and most dark particulates pool on the pond bottom decreasing its albedo (Light et. al., 1998; Nürnberg et. al., 1994). Furthermore, most of the solar energy absorbed by the large body of fresh water will be deposited at the bottom, melting the points on the bottom quickly. However, we believe that even stopping pond growth might be enough to explain the observations.

We saw that bottom melting makes it harder for points on the pond edge to move upwards. If there
370 is less bottom melting, the requirements for the dichotomy are looser. Sunlight entering the ocean
through the leads is the main source of the bottom heat flux (Maykut and Mcphee, 1995). Bottom
melting is thus highly correlated with the ice concentration (Perovich et. al., 2011), which means that
the dichotomy may more likely be observed in regions of high ice concentration, if the mechanism
for bimodality described here is correct.

375 We showed that the timescale of pond growth or shrinkage is unconstrained since it depends on
the slope of the ice-water interface. As time progresses, the slope of the ice at the edge of the ponds
generally steepens (Fetterer et. al., 1998). This means that the ponds should eventually stop shrinking
or growing. This model would therefore tend to suggest that growth or shrinkage mostly occurs only
in the early stages of the melt.

380 Observations do not offer conclusive evidence that the melt pond dichotomy is real. The floes
with small pond coverage could be a part of continuous distribution in pond coverage which is not
resolvable due to a small number of observations. We already mentioned that a long tailed unimodal
distribution can be produced if part of the initial distribution is near a fixed point (Fig. 8). There
probably exist other mechanisms that can achieve this as well (e.g. the timescale (Eq. (13)), need
385 not be the same for every floe, and this variation in the timescale could lead to broadening of the
final pond coverage distribution). Nevertheless, we have shown here that under certain conditions
the dichotomy can be physical, and produced by the mechanism we describe. Our model showed
how important the boundary layer between ice and pond is, and how a small subset of points could
be governing the entire evolution of the system.

390 Landy et. al. (2014) describe field observations of melt ponds in the Canadian Arctic in 2011 made
on landfast first year sea ice. They set up a rectangular observation area with a side length of $50\mathrm{m}$,
and observed melt pond evolution via LIDAR located at the four corners of the observation area.
They observed a freeboard drop of $3\mathrm{cm}$ between June 22nd and June 26th, and the new areas that
became ponded on June 26th were those which were $3\mathrm{cm}$ above sea level on June 22nd. This means
395 that points on the pond edge melted at roughly the same rate as points on bare ice ($k \approx 1$), which is
an argument against our bimodal mechanism. This is, however, only a single case study. It would be
best if such observations were made on pond-free floes.

Even if the mechanism described here does not explain the dichotomy in the Arctic sea ice, it
could still operate under different conditions. For example, it was hypothesized that during Snowball
400 Earth events there was a layer of dirty ice near the equator (Abbot et. al., 2010). Here, the effect of
washing out dark particulates would be especially important. This could have promoted a dichotomy
of hypothetical melt ponds near the equator. It might be interesting to investigate how the ponds
would have evolved as the Snowball warmed and deglaciated.

6 Conclusions

405 Observations of Arctic first year sea ice suggest a dichotomy in melt pond coverage: while some floes become heavily ponded, others remain hardly ponded. Here we presented a conceptual model to explain these observations. We showed that if some points on the ice melt slower than the others, they can actually move upwards while the ice is melting. In this way ponds can shrink if points on their perimeter move upwards. Whether they will move upwards (ponds shrink) or downwards 410 (ponds grow) depends on the magnitudes of melting above and below sea level, and since ponded ice is below sea level, on the pond fraction. If the points near the pond perimeter melt slowly enough, an unstable fixed point in pond coverage emerges, such that the evolution of ponds depends on whether the initial pond coverage is above or below this threshold. A floe either becomes heavily ponded or non ponded, potentially explaining the dichotomy. In this way, we showed how a narrow 415 boundary between bare ice and melt ponds can govern the subsequent evolution of the entire ice floe. We presented a single-column model of pond evolution, and showed that this evolution happens on relevant timescales. We also presented a 2D generalization of this model, and showed that it behaves qualitatively similar to the simple model, with the only noticeable difference being that ponds do not disappear, but shrink a little and then get deeper and deeper. In order to test our theory we need more 420 observational data, or detailed physical theories at the micro scale. If the theory proves to be correct in describing the dichotomy, it will be the first step in assessing the impact of this phenomenon on the total albedo of the ice pack, and its role in a changing global climate.

Appendix A: Evaluating the dimensionless perimeter function $p_0(x)$

We evaluated the dimensionless perimeter function $p_0(x)$ by generating a synthetic topography and 425 truncating it by a plane. Ponds were defined as regions of the topography below the plane, and bare ice as regions above the plane. Then, by lifting the plane we tracked the total area and the total perimeter of the ponds, thus defining the function $p_0(x)$. The synthetic topography was created from a Fourier power spectrum, $P(\mathbf{k})$. For each point $\mathbf{r}$ the height of the topography, $H(\mathbf{r})$, is the real part of the inverse Fourier transform,

430
$$H(\mathbf{r}) = Re\Big(\sum_{k_x,k_y} P(\mathbf{k}) e^{-i\mathbf{k}\mathbf{r}+\phi} \Big). \tag{A1}$$

The phase ϕ is a random number from 0 to 2π, making the topography random. We defined the power spectrum as, $P(\mathbf{k}) = P_0\Theta(|\mathbf{k}| - k_0)$, where Θ is the step function equal to unity when its argument is positive and zero otherwise. The constant k_0 thus defines the length scale of the typical pond as $l_0 = \frac{2\pi}{k_0}$. By knowing l_0 and the area of the image in pixels we can infer the dimensionless 435 perimeter as $p_0(x) = P(x)\frac{l_0}{A}$, where $P(x)$ is the total number of pixels on the perimeters of ponds for a particular bare ice fraction x (ratio of the numbers of non ponded pixels to all pixels). Figure 11 shows an example of one topography and the resulting melt pond configurations for different sea

level heights (left panel) as well as the dimensionless perimeter function obtained in this way (right panel). Topography created in this way probably does not represent sea ice realistically, but for our illustrative purposes it is good enough, especially since the shape of the dimensionless perimeter function does not affect the qualitative behavior of bare ice fraction in our model.

440

Acknowledgements. We thank B. Cael Barry, Daniel Koll, Edwin Kite, and Mary Silber for reading the paper and giving useful comments. We also thank Douglas MacAyeal, and Edwin Kite for discussions and ideas about the physical mechanisms involved.

References

445

Abbot, D. S., and Pierrehumbert, R. T.: Mudball: Surface dust and Snowball Earth deglaciation., J. Geophys. Res., 115(D03), doi:10.1029/2009JD012007, 2010.

Abbot, D. S., Silber, M., and Pierrehumbert, R. T.: Bifurcations leading to summer Arctic sea ice loss, J. Geophys. Res., 116(D19), 2011.

450 Arrigo, K. R., D. K. Perovich, R. S. Pickart, Z. W. Brown, G. L. Van Dijken, K. E. Lowry, M. M. Mills, M. A. Palmer, W. M. Balch, F. Bahr, N. R. Bates, C. Benitez-Nelson, B. Bowler, E. Brownlee, J. K. Ehn, K. E. Frey, R. Garley, S. R. Laney, L. Lubelczyk, J. Mathis, A. Matsuoka, B. G. Mitchell, G. W. K. Moore, E. Ortega-Retuerta, S. Pal, C. M. Polashenski, R. A. Reynolds, B. Schieber, H. M. Sosik, M. Stephens, and J. H. Swift.: Massive Phytoplankton Blooms Under Arctic Sea Ice, Science, 336, 6087, doi:10.1126/science.1215065.

455 2012.

Eicken, H., Grenfell, T. C., Perovich, D. K., Richter-Menge, J. A., and Frey, K.: Hydraulic controls of summer Arctic pack ice albedo, J. Geophys. Res., 109(C8), doi:10.1029/2003jc001989, 2004.

Eisenman, I. and Wettlaufer, J. S.: Nonlinear threshold behavior during the loss of Arctic sea ice, Proceedings of the National Academy of Sciences, 106(1), 28–32, doi:10.1073/pnas.0806887106, 2008.

460 Fetterer, F., and Untersteiner, N.: Observations of melt ponds on Arctic sea ice, J. Geophys. Res., 103(C11), 24821, doi:10.1029/98jc02034, 1998.

Flocco, D., Feltham, D. L. and Turner, A. K.: Incorporation of a physically based melt pond scheme into the sea ice component of a climate model, J. Geophys. Res., 115(C8), doi:10.1029/2009jc005568, 2010.

Frey, K. E., Perovich, D. K. and Light, B.: The spatial distribution of solar radiation under a melting Arctic sea

465 ice cover, Geophys. Res. Lett., 38(22), doi:10.1029/2011gl049421, 2011.

Hohenegger, C., Alali, B., Steffen, K. R., Perovich, D. K., and Golden, K. M.: Transition in the fractal geometry of Arctic melt ponds, The Cryosphere, 6, 1157-1162, doi:10.5194/tc-6-1157-2012, 2012.

Holland, M. M., Bitz, C. M. and Tremblay, B.: Future abrupt reductions in the summer Arctic sea ice, Geophys. Res. Lett., 33(23), doi:10.1029/2006gl028024, 2006.

470 Holland, M. M., Bailey, D. A., Briegleb, B. P., Light, B. and Hunke, E.: Improved Sea Ice Shortwave Radiation Physics in CCSM4: The Impact of Melt Ponds and Aerosols on Arctic Sea Ice*, J. Climate, 25(5), 1413–1430, doi:10.1175/jcli-d-11-00078.1, 2012.

Landy, J., Ehn, J., Shields, M., and Barber, D.: Surface and melt pond evolution on landfast first-year sea ice in the Canadian Arctic Archipelago, J. Geophys. Res. Oceans, 119(5), 3054–3075, doi:10.1002/2013jc009617,

475 2014.

Landy, J. C., Ehn, J. K. and Barber, D. G.: Albedo feedback enhanced by smoother Arctic sea ice, Geophys. Res. Lett., doi:10.1002/2015gl066712, 2015.

Light, B., Eicken, H., Maykut, G. A., and Grenfell, T. C.: The effect of included participates on the spectral albedo of sea ice, J. Geophys. Res., 103(C12), 27739, doi:10.1029/98jc02587, 1998.

480 Makshtas, A. P. and Podgorny, I. A.: Calculation of melt pond albedos on Arctic sea ice, Polar Research, 15(1), doi:10.3402/polar.v15i1.6635, 1996.

Maykut, G. A. and Mcphee, M. G.: Solar heating of the Arctic mixed layer, J. Geophys. Res., 100(C12), 24691–24691, doi:10.1029/95jc02554, 1995.

Morassutti, M. P. and Ledrew, E. F.: Albedo And Depth Of Melt Ponds On Sea-Ice, Int. J. Climatol., 16(7),
485   817–838, doi:10.1002/(SICI)1097-0088(199607)16:7<817::AID-JOC44>3.0.CO;2-5, 1996.

Nicolaus, M., Katlein, C., Maslanik, J. and Hendricks, S.: Changes in Arctic sea ice result in increasing light
transmittance and absorption, Geophys. Res. Lett., 39(24), doi:10.1029/2012gl053738, 2012.

North, G.R.: The Small Ice Cap Instability in Diffusive Climate Models, Journal of the Atmospheric Sciences,
41(23), 3390-3395, 1984.

490   Nürnberg, D., Wollenburg, I., Dethleff, D., Eicken, H., Kassens, H., Letzig, T., Reimnitz, E. and Thiede, J.:
Sediments in Arctic sea ice: Implications for entrainment, transport and release, Marine Geology, 119(3-4),
185–214, doi:10.1016/0025-3227(94)90181-3, 1994.

Pedersen, C. A., Roeckner, E., Lüthje, M. and Winther, J. G.: A new sea ice albedo scheme including melt ponds
for ECHAM5 general circulation model, J. Geophys. Res., 114(D8), doi:10.1029/2008jd010440, 2009.

495   Perovich, D. K.: The Optical Properties of Sea Ice, No. MONO-96-1. Cold Regions Research and Engineering
Lab Hannover NH, 1996.

Perovich, D. K., and Polashenski, C.: Albedo evolution of seasonal Arctic sea ice, Geophys. Res. Lett., 39(8),
doi:10.1029/2012gl051432, 2012.

Perovich, D. K. and Richter-Menge, J. A.: Loss of Sea Ice in the Arctic*. Annu. Rev. Marine. Sci., 1(1),
500   417–441. doi:10.1146/annurev.marine.010908.163805, 2009.

Perovich, D. K., Roesler, C. S., and Pegau, W. S.: Variability in Arctic sea ice optical properties, J. Geophys.
Res., 103(C1), 1193, doi:10.1029/97jc01614, 1998.

Perovich, D. K., Tucker, W. B., and Ligett, K. A.: Aerial observations of the evolution of ice surface conditions
during summer, J. Geophys. Res., 107(C10), doi:10.1029/2000jc000449, 2002.

505   Perovich, D. K., Thomas, C. G., Richter-Menge, J. A., Light, B., Tucker, W. B., and Eicken, H.:
Thin and thinner: Sea ice mass balance measurements during SHEBA, J. Geophys. Res., 108(C3),
doi:10.1029/2001jc001079, 2003.

Perovich, D. K., Light, B., Eicken, H., Jones, K. F., Runciman, K. and Nghiem, S. V.: Increasing solar heating
of the Arctic Ocean and adjacent seas, 1979–2005: Attribution and role in the ice-albedo feedback, Geophys.
510   Res. Lett., 34(19), doi:10.1029/2007gl031480, 2007.

Perovich, D. K., Richter-Menge, J. A., Jones, K. F., Light, B., Elder, B. C., Polashenski, C., Laroche, D.,
Markus, T., Lindsay, R.: Arctic sea-ice melt in 2008 and the role of solar heating, Annals of Glaciology,
52(57), 355–359, doi:10.3189/172756411795931714, 2011.

Pfirman, S., Lange, M. A., Wollenburg, I. and Schlosser, P.: Sea Ice Characteristics and the Role of Sediment In-
515   clusions in Deep-Sea Deposition: Arctic — Antarctic Comparisons, Geological History of the Polar Oceans:
Arctic versus Antarctic, 187–211, doi:10.1007/978-94-009-2029-3_11, 1990.

Polashenski, C., Perovich, D., and Courville, Z.: The mechanisms of sea ice melt pond formation and evolution,
J. Geophys. Res., 117(C1). doi:10.1029/2011jc007231, 2012.

Scott, F. and Feltham, D. L.: A model of the three-dimensional evolution of Arctic melt ponds on first-year and
520   multiyear sea ice, J. Geophys. Res., 115(C12), doi:10.1029/2010jc006156, 2010.

Screen, J. A. and Simmonds, I.: The central role of diminishing sea ice in recent Arctic temperature amplifica-
tion, Nature, 464(7293), 1334–1337, doi:10.1038/nature09051, 2010.

Serreze, M. C., and Stroeve, J.: Arctic sea ice trends, variability and implications for seasonal ice forecasting, Phil. Trans. R. Soc. A, 373(2045), 20140159, doi:10.1098/rsta.2014.0159, 2015.

525 Stroeve, J., Holland, M. M., Meier, W., Scambos, T. and Serreze, M.: Arctic sea ice decline: Faster than forecast, Geophys. Res. Lett., 34(9), doi:10.1029/2007gl029703, 2007.

Strogatz, S. H.: Nonlinear dynamics and chaos with applications to physics, biology, chemistry, and engineering, Westview Press, Cambridge, MA., 2000.

Tucker, W. B., Gow, A. J., Meese, D. A., Bosworth, H. W. and Reimnitz, E.: Physical characteristics of summer 530 sea ice across the Arctic Ocean, J. Geophys. Res., 104(C1), 1489–1489, doi:10.1029/98jc02607, 1999.

Webster, M. A., Rigor, I. G., Perovich, D. K., Richter-Menge, J. A., Polashenski, C. M., and Light, B.: Seasonal evolution of melt ponds on Arctic sea ice, J. Geophys. Res. Oceans, 120(9), 5968–5982, doi:10.1002/2015jc011030, 2015.

Yackel, J. J., Barber, D. G. and Hanesiak, J. M.: Melt ponds on sea ice in the Canadian Archipelago: 535 1. Variability in morphological and radiative properties, J. Geophys. Res., 105(C9), 22049–22049, doi:10.1029/2000jc900075, 2000.

Zhang, J., Lindsay, R., Steele, M. and Schweiger, A.: What drove the dramatic retreat of arctic sea ice during summer 2007?, Geophys. Res. Lett., 35(11), doi:10.1029/2008gl034005, 2008.
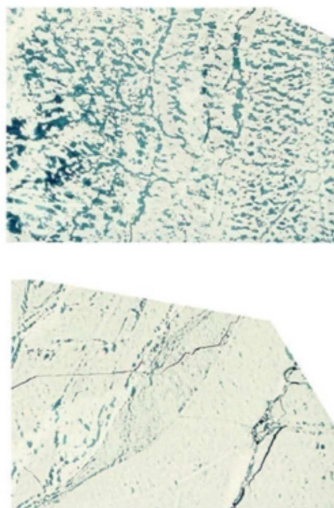
Figure 1. Images of two different ice floes taken at the same time at the height of the melt season and close to each other. One is heavily ponded, while other only slightly ponded. This figure is taken from Perovich et. al. (2002)
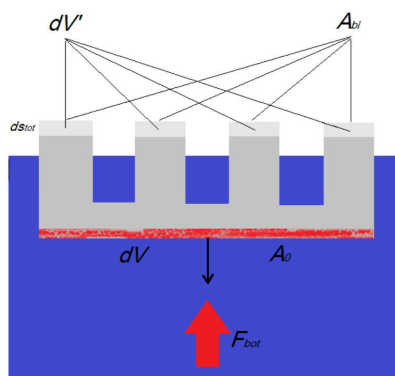
Figure 4. Hydrostatic adjustment. Ice is melting from below by ocean heat flux F_{bot}. After some time an area, A_0, of some thickness melts (red region), which corresponds to a volume $dV = \frac{F_{\mathrm{bot}} A_0 \, dt}{L}$. This has to be followed by sinking of the ice above sea level. Because ice can only cross sea level in places where its surface is above sea level, the change in ice volume above sea level (dV', light gray region), after sinking by ds_{tot}, is proportional to the area of bare ice (A_{bi}). Hydrostatic adjustment then requires $dV' = \frac{\rho_{\mathrm{w}} - \rho_{\mathrm{i}}}{\rho_{\mathrm{w}}} dV$. Here, we are neglecting the effect of ponds growing while the ice is sinking, since it is a second order effect on the hydrostatic adjustment.
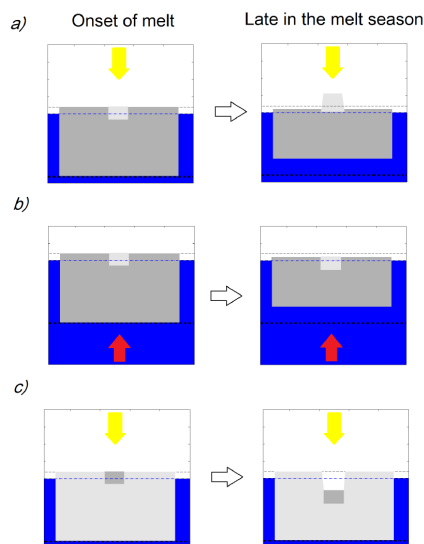
Figure 2. Different ways to melt the ice. Left panels show a slab of ice before the onset of melt. Right panels show the slab later in the melt season. a) Rigid body displacement - melting above sea level. A slab of ice is floating in water (blue) and melting from above by sunlight. The dark gray represents ice with a low albedo that melts, while lighter gray represents perfectly reflective ice that does not melt. After some time, the perfectly reflective region has moved upwards relative to its location at the beginning because the ice around it has melted, removing mass above sea level. Black dashed lines show the position of top and bottom of the ice on day 0, and the blue dashed line represents sea level. b) Rigid body displacement - melting below sea level. Ice (dark gray) is melting from below. After some time, the surface of the ice sinks regardless of its characteristics. The reflective region is no different, and moves downwards because ice beneath it has melted removing mass below sea level. c) Local melting. Ice is melting from above by sunlight. Most of the ice is perfectly reflective and does not melt (light gray), apart from a small region of ice that does melt (dark gray). After some time, most of the ice remains unchanged, but the special region melts to below sea level. The region of enhanced melt has moved downwards because it itself has melted.
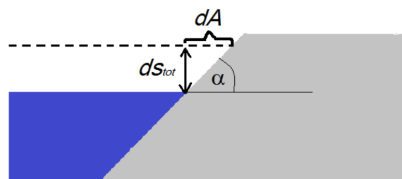
Figure 5. Relating the vertical displacement to the change in area of melt ponds. The dashed line represents the new water level relative to ice, after it has sunk by ds_{tot}. The area of the melt ponds changes by $dA = ds_{\text{tot}}\cot(\alpha)P$, where α is the slope between ice and water and P is the perimeter of the ponds.
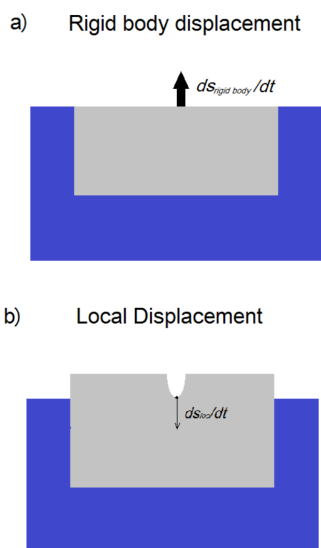
Figure 3. a) Rigid body displacement represents the motion of the floe as a whole in an effort to maintain hydrostatic balance because melting removes mass above or below sea level. Melting above sea level induces an upward motion of the floe, whereas melting below sea level induces a downward motion. b) Local displacement represents the movement of a point on the ice surface as a result of ice melting at that particular point. It is a function only of local ice characteristics at that point. For both local and rigid body displacements the positive direction is defined as upwards.
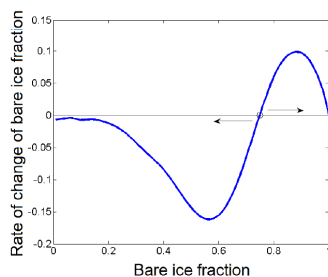
Figure 6. Phase portrait for the bare ice fraction. The bare ice fraction is represented on the x-axis, and its rate of change on the y-axis. The circle represents the unstable fixed point. Fluctuations at low bare ice fractions are numerical artifacts, and are a result of the way we estimated the function $p_0(x)$ (see appendix A). If the initial bare ice fraction is less than the fixed point, its rate of change is negative, and the bare ice fraction decreases. If the initial bare ice fraction is greater than the fixed point, its rate of change is positive, the bare ice fraction grows, and the floe gets less and less ponded. The initial bare ice fraction refers to the bare ice fraction at the time when ice first becomes permeable.
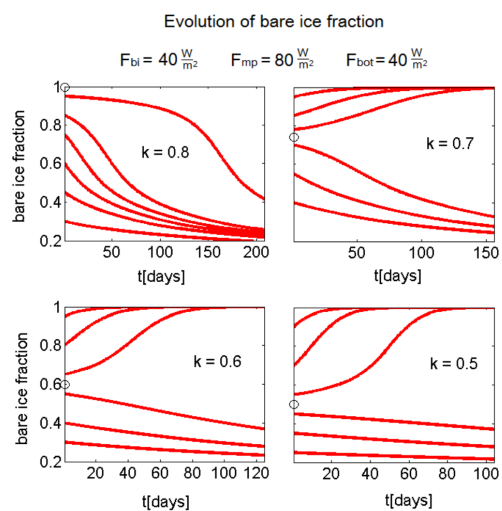
Figure 7. Numerical solution of Eq. (9) for several different initial conditions and several different ratios of perimeter to bare ice melting, k. Circles represent locations of the fixed points. If the points on the perimeter melt 20% slower than average, the fixed point is physical and the dichotomy in melt pond coverage can be explained by this mechanism. Changes happen on the timescales of about one or two months, which is comparable to the timescale of the melt season
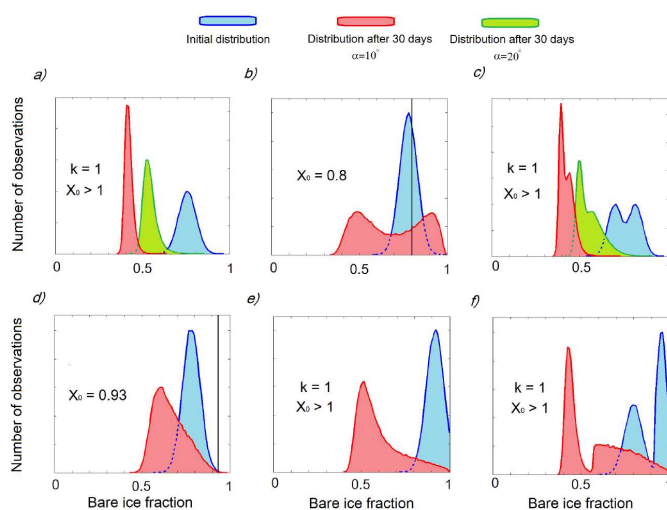
Figure 8. In this figure we have evolved an ensemble of 10^5 floes with a slope $\alpha = 10^o$ and some initial distribution of bare ice fractions according to Eq. (9). Blue curves represent the initial bare ice fraction distribution, while the red and green curves represent the bare ice fraction distribution after 30 days. Green curves, where they exist, correspond to a steeper slope of $\alpha = 20^o$. Alternatively they could be viewed as having the same slope as the red curves, but corresponding to an earlier time. Vertical black lines represent the locations of fixed points. We consider cases with $0 < x_0 < 1$ as well as $k = 1$ (meaning $x_0 > 1$). a) Points on the perimeter of the ponds melt at the same rate as bare ice, $k = 1$, and there is no nontrivial fixed point. As time passes, the distributions become narrower and narrower, with all the floes having very similar pond fractions. b) A fixed point at $x_0 = 0.8$ splits the initial distribution into two parts of comparable area. After 30 days, floes follow a bimodal distribution. c) The initial distribution is bimodal and $k = 1$. Bimodality diminishes with time as the distribution becomes more localized. d) A fixed point at $x_0 - 0.93$ does not split the initial distribution. The distribution evolves to become unimodal and long tailed e) The initial distribution close to the trivial fixed point at $x = 1$ with $k = 1$ evolves to become unimodal and long tailed f) The initial distribution is bimodal with one of the modes close to $x = 1$. $k = 1$.
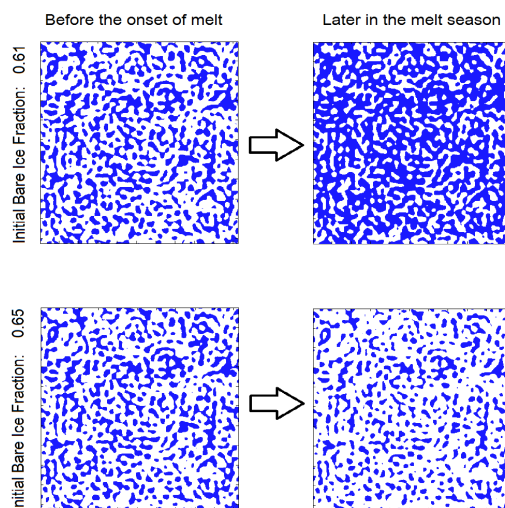
Figure 9. Evolution of 2D surfaces. The upper surface is identical to the lower surface apart from it being slightly more ponded. After evolving the surfaces for some time the upper one gets heavily ponded, while the pond coverage on the lower one decreases. A noticeable difference between this and the single-column model is that in the 2D case, the ponds cannot disappear. They shrink a little, and then get deeper and deeper without shrinking or growing.
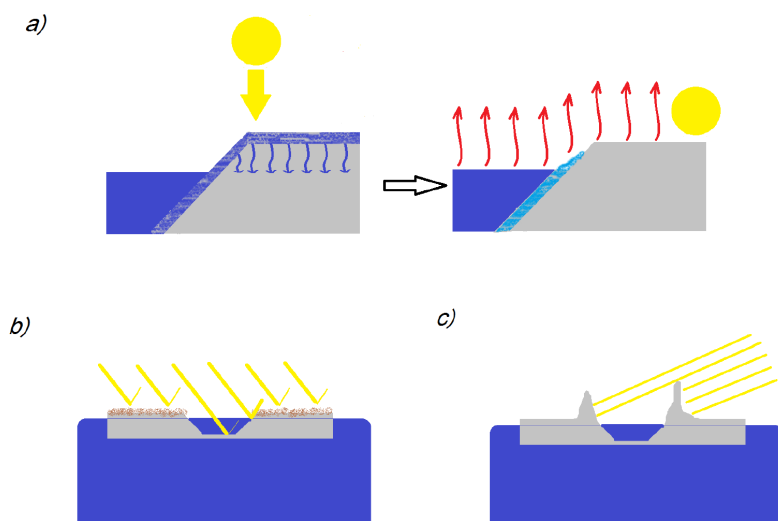
Figure 10. Processes that might lead to ice at the pond edge melting slower than bare ice a) If ice melts during one part of the day and freezes during another, meltwater could seep through the bare ice. There would be no water to freeze on bare ice during the freezing part of the day, but there could be freezing near the pond edge. This could make the pond edge effectively melt more slowly. b) Inclusion of dark impurities, such as soot, dust, or sediments, could lower the albedo of bare ice. Pond water could wash away the dirt, making the pond edge more reflective. c) The pond is at a lower elevation than any of the points on bare ice causing it to receive less sunlight than bare ice. This is especially pronounced on rough ice where ridges could provide effective shading.
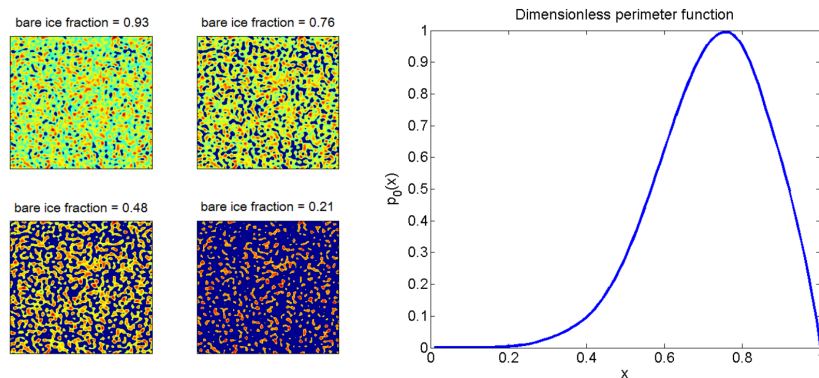
Figure 11. Left panel: random topography created from a Fourier power spectrum and filled to a certain height. Dark blue regions represent ponds and correspond to regions of the topography below fill level, and the colored regions represent bare ice. Color stands for height above sea level. Right panel: Dimensionless perimeter as a function of bare ice fraction obtained from the topography in the left panel by rising the sea level. We see that the function has the expected shape: it is positive, of the order unity, and goes to zero as x goes to either zero or one.